

AN ANALYTICAL MODEL FOR STEEL SHEAR WALL STRENGTHENED WITH CFRP USING COMPOSITE THEORY

Majid GHOLHAKI

*Assistant Professor, Semnan University, Semnan, Iran
mgholhaki@semnan.ac.ir*

Younes NOURI

*M. Sc Student, Ferdowsi University, Mashhad, Iran
Nouri.Younes@stu.um.ac.ir*

Keywords: Composite Steel Shear Wall, CFRP, Diagonal Tension Field, Virtual Work, Elastic Strength

ABSTRACT

In this paper steel plate shear wall strengthen by Carbon Polymer's Fiber was studied. An equation has been proposed for elastic strength using composite theory and maximum work failure model, and another equation has been obtained for elastic displacement related to polymer's fiber using virtual work principle. Considering fibers and shear wall web as a layer and super positioning plate and fiber behavior, composite shear wall model was achieved. Optimum fiber orientation angle for composite shear wall was in diagonal tension field. Finite element values via presented model was compared with and concluded that the offered model can predict composite shear wall in close range.

INTRODUCTION

Steel shear wall can significantly tackle and tolerate lateral loads due to wind and earthquake through diagonal tension field of steel plates confined between boundary elements of system (Astaneh –Asl 2001). The first philosophy of steel shear wall design was based on preventing global buckling in plate, however, it was later seen that most of post shear strength of shear wall was achieved after buckling of plate (Wagner 1931, Takahashi 1973). These shear walls were initially utilized as a retrofit system, however, after their good performance was approved, they were applied as a structure system. Some advantages of this system are high ductility, energy absorption, stiffness and strength, on contrary the disadvantage of this system is low elastic strength of steel walls. To improve shear performance of steel shear walls, adding vertical and horizontal stiffeners (Takahashi 1973), low yield point plate materials (Kharrazi 2005), strengthening with concrete (Vian 2004, Rahai 2009, Arabzadeh 2011), perforated web plate (Vian 2004) and covering steel plate with FRP materials (Hatami 2012, Nategh-Alahi 2012, Rahai 2011) have been studied. Due to light weight, high elasticity module and high tension strength, FRP materials have a wide application in civil engineering. Covering plate with FRP increases the shear strength, energy absorption, excessive post buckling field distribution and stiffness of shear wall. So far, configuration of fiber orientation, behavior and seismically parameters of composite steel shear wall have been evaluated by numerical and empirical methods (Nateghi-Alahi 2012) and yet no explicit analytical method has been presented, but experimental and numerical studies absolutely depend on dimension and mechanical properties of steel and FRP. Two major analytical methods have been presented for analysis of steel shear wall that are stripe model (Thorburn 1983) and plate and frame interaction (Roberts 1991). Plate – frame interaction in most cases yields the precise values. In Rahai and Hatami (2012), some specimen strengthened with CFRP layers have been studied and in these experimental tests, fiber orientations, thickness of CFRP and shear wall dimension under cyclic loading were evaluated. Finally, some equations were proposed for nonlinear behavior of CSSW using elastic analysis. In Rahai and Alipour (2011) evaluated the ductility, stiffness, yield shear force factors under push over analysis as well as thickness of FRP layers and conclude that in diagonal tension field,

overall strength and stiffness of shear wall have been increased. In addition, Nateghi-Alahi and Khazaei-Poul (2012) conducted five experimental tests on composite steel shear wall under cyclic loading, different fiber angle and thickness. They concluded that fiber inclination is the most important variable on behavior of composite shear wall, moreover, they concluded that initial and secant stiffness of CSSW would increase if principal orientation of fiber material is in tension filed angle. In this article, over-strength and seismic parameter of composite steel plate shear wall, strengthened with FRP materials using analytical and almost simple methods, have been studied. Furthermore, stress and strain in FRP material in different fiber angles, extra strength due to FRP, stiffness of shear wall after adding FRP and Elastic shear displacement in FRP were achieved using these equations.

VERIFICATION

According to F. Nateghi-Alahi and M. khazaei (2012), to calibrate FEM software, an experimental test was selected and simulated with FEM software. In experimental test, CSPSP3 was chosen because it is strengthened with one layer FRP on each side at fiber orientation 45/-45 degree. This specimen is more consistent with FEM simulation of this study. The numerical push-over curve for both FEM and Experimental tests are presented and compared in Fig .1. It is concluded that FEM Simulation has been successful in estimating the shear capacity and behavior of CSPSP3.

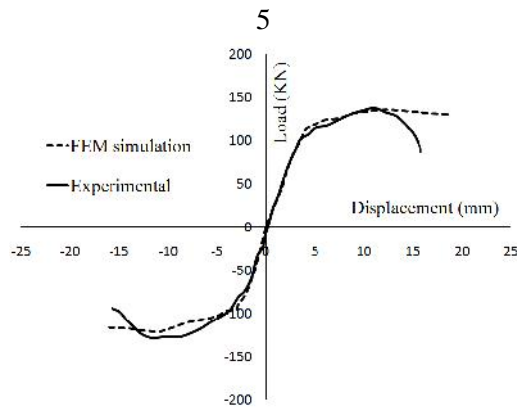


Fig .1 Good agreement of Experimental and FEM simulation

COMPOSITE STRUCTURAL ANALYSIS

The analysis of composite structures is more complicated than that of conventional metallic structures. While metallic structures can usually be treated as isotropic materials, in which the properties do not depend on orientation, composite materials are not homogeneous and are anisotropic in nature. The 1-2 system is known as the principal material axes system, with the 1-direction parallel or longitudinal to the fiber direction (zero-degree) and the one-direction perpendicular or transverse to the fiber direction (90-degree). the second system, represented by x-y, is the structural loading direction or the direction in which loads are applied to the ply. The angle between the x-axis and the 1-axis is called the fiber orientation angle. The stresses in the structural axes (\dagger_{xx} , \dagger_{yy} , and \dagger_{xy}) can be obtained from those in the material axes (\dagger_{11} , \dagger_{22} , and \dagger_{12}) by equation 1, (Valery 2001, Jones 1999).

$$\begin{bmatrix} \dagger_{xx} \\ \dagger_{yy} \\ \dagger_{xy} \end{bmatrix} = \begin{bmatrix} m^2 & n^2 & -2mn \\ n^2 & m^2 & 2mn \\ mn & -mn & m^2 - n^2 \end{bmatrix} \begin{bmatrix} \dagger_{11} \\ \dagger_{22} \\ \dagger_{12} \end{bmatrix} \quad 1$$

where $m=\cos\theta$ and $n=\sin\theta$. Fig .2 presents the stress in structural axes and material axes. Similarly, the strain in material axes can be transformed to structural axes by equation 2.

$$\begin{bmatrix} V_{xx} \\ V_{yy} \\ X_{xy} \end{bmatrix} = \begin{bmatrix} m^2 & n^2 & -mn \\ n^2 & m^2 & mn \\ 2mn & -2mn & m^2 - n^2 \end{bmatrix} \begin{bmatrix} V_{11} \\ V_{22} \\ X_{12} \end{bmatrix} \quad 2$$

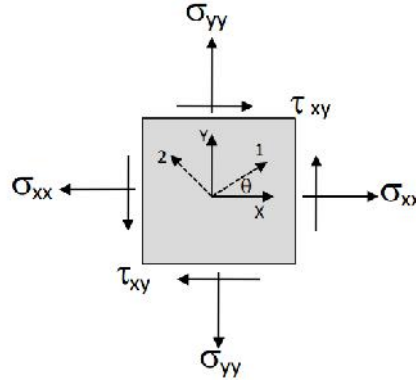


Fig .2 stress in structural and materials axes

The Stress-Strain relationship for a single ply, loaded by off-axis to the material was obtained from Eq. (3).

$$\begin{bmatrix} \dagger_{xx} \\ \dagger_{yy} \\ \dagger_{xy} \end{bmatrix} = \begin{bmatrix} \overline{Q_{11}} & \overline{Q_{12}} & \overline{Q_{16}} \\ \overline{Q_{21}} & \overline{Q_{22}} & \overline{Q_{26}} \\ \overline{Q_{16}} & \overline{Q_{26}} & \overline{Q_{66}} \end{bmatrix} \begin{bmatrix} V_{xx} \\ V_{yy} \\ X_{xy} \end{bmatrix} \quad 3$$

where \$[Q]\$ is stiffness matrix and \$[\overline{Q}]\$ is stiffness coefficient. The elements of \$[\overline{Q}]\$ are defined as Eqs. (4)-(9).

$$\overline{Q_{11}} = U_1 + U_2 \cos 2\theta + U_3 \cos 4\theta \quad 4$$

$$\overline{Q_{12}} = \overline{Q_{21}} = U_4 - U_3 \cos 4\theta \quad 5$$

$$\overline{Q_{16}} = 1/2U_2 \sin 2\theta + U_3 \sin 4\theta \quad 6$$

$$\overline{Q_{22}} = U_1 - U_2 \cos 2\theta + U_3 \cos 4\theta \quad 7$$

$$\overline{Q_{26}} = 1/2U_2 \sin 2\theta - U_3 \sin 4\theta \quad 8$$

$$\overline{Q_{66}} = U_5 - U_3 \cos 4\theta \quad 9$$

Where \$U_1\$ through \$U_5\$ obtained from Eqs. (10)-(14).

$$U_1 = 1/8(3\overline{Q_{11}} + 3\overline{Q_{22}} + 2\overline{Q_{12}} + 4\overline{Q_{66}}) \quad 10$$

$$U_2 = 1/2(\overline{Q_{11}} - \overline{Q_{22}}) \quad 11$$

$$U_3 = 1/8(\overline{Q_{11}} + \overline{Q_{22}} + 2\overline{Q_{12}} - 4\overline{Q_{66}}) \quad 12$$



$$U_4 = 1 / 8 (3Q_{11} + 3Q_{22} + 6Q_{12} - 4Q_{66}) \quad 13$$

$$U_5 = 1 / 2 (U_1 - U_4) \quad 14$$

And also elements of [Q] matrix defined as Eqs. (15)-(18)

$$Q_{11} = \frac{E_1}{1 - \nu_{12}\nu_{21}} \quad 15$$

$$Q_{12} = \frac{\nu_{21}E_1}{1 - \nu_{12}\nu_{21}} \quad 16$$

$$Q_{22} = \frac{E_2}{1 - \nu_{12}\nu_{21}} \quad 17$$

$$Q_{66} = G_{12} \quad 18$$

The relationship between major Poisson's ratio and minor Poisson's ratio is expressed as Eq. (19).

$$\frac{\nu_{12}}{E_{11}} = \frac{\nu_{21}}{E_{22}} \quad 19$$

The elastic constants for an angle ply or off-axis ply can be calculated using Eq. (20)-(24).

$$E_{yy} = \left[\frac{n^4}{E_{11}} + \left(\frac{1}{G_{12}} - \frac{2\nu_{12}}{E_{11}} \right) m^2 n^2 + \frac{m^4}{E_{22}} \right]^{-1} \quad 20$$

$$E_{xx} = \left[\frac{m^4}{E_{11}} + \left(\frac{1}{G_{12}} - \frac{2\nu_{12}}{E_{11}} \right) m^2 n^2 + \frac{n^4}{E_{22}} \right]^{-1} \quad 21$$

$$G_{xy} = \left[\left(\frac{4}{E_{11}} + \frac{4}{E_{22}} + \frac{8\nu_{12}}{E_{11}} - \frac{2}{G_{12}} \right) \frac{m^2 n^2}{E_{11}} + \left(\frac{m^4 + n^4}{G_{12}} \right) \right]^{-1} \quad 22$$

$$\nu_{xy} = E_{xx} \left[\frac{\nu_{12}(m^4 + n^4)}{E_{11}} - \left(\frac{1}{E_{11}} + \frac{1}{E_{22}} - \frac{1}{G_{12}} \right) m^2 n^2 \right] \quad 23$$

$$\nu_{yx} = \nu_{xy} \frac{E_{yy}}{E_{xx}} \quad 24$$

FAILURE THEORIES

Failure prediction for metallic structures is normally performed by comparing stresses or strains caused by applied loads with the allowable strength or strain capacity of the material. For isotropic materials that exhibit yielding, either the Tresca maximum shear stress theory or von Mises distortional energy theory is commonly used. However, composites are not isotropic and they do not yield. Failure modes in composites are generally noncatastrophic and may involve localized damage via such mechanisms as fiber breakage,



matrix cracking, debonding, and fiber pull-out. These can progress simultaneously and interactively, making failure prediction for composite complexes. There are five independent strength constants that are important for a single ply. S_{Lt} or V_{Lt} - longitudinal tensile strength or strain, S_{Tt} or V_{Tt} - transverse tensile strength or strain, S_{Lc} or V_{Lc} - longitudinal compressive strength or strain, S_{Tc} or V_{Tc} - transverse compressive strength or strain, S_s or χ_s - in-plane shear strength or strain.

Maximum Stress Criterion. According to this theory, failure occurs when any stress in the principal material directions is equal to or greater than the corresponding allowable strength.

Maximum Strain Theory. The maximum strain theory is very similar to the maximum stress theory except that strains are used instead of stresses. According to this theory, failure will occur if any strain in the principal material axes is equal to or greater than the corresponding allowable strain.

Azai-Tsai-Hill Maximum Work theory. the maximum work theory states that for plane stress, failure initiates when the inequality Eq. 25 is violated.

$$\frac{\sigma_{11}^2}{S_{Lt}^2} - \frac{\sigma_{11}\sigma_{22}}{S_{Lt}^2} + \frac{\sigma_{22}^2}{S_{Tt}^2} + \frac{\tau_{12}^2}{S_s^2} < 1 \quad 25$$

The advantage of the Azai-tsai-Hill criterion is that the interaction between strengths and failure modes is taken into account.

SPSW - FRP COMPOSITE MODEL

OPTIMUM FIBER ORIENTATION ANGLE

Based on FE models and reports on Nateghi-Alahi (2012), if principal orientation of FRP layers is oriented in the direction of diagonal tension field, the shear strength and stiffness of composite shear wall will increase. Because tensile strength in principal direction of FRP is greater than transverse tensile strength, then placing main fiber direction in diagonal tension of plate increases shear strength and stiffness of composite shear wall.

FRP ELASTIC SHEAR STRENGTH

Using Eq. (1) and assuming that σ_{xx} and σ_{yy} are negligible in fiber element, the stresses in fiber element written as Eqs. (26)-(28).

$$\sigma_{11} = 2mn\tau_{xy} \quad 26$$

$$\sigma_{22} = -2mn\tau_{xy} \quad 27$$

$$\tau_{12} = (m^2 - n^2)\tau_{xy} \quad 28$$

Substitution of equation 27, 28, and 29 into 26 yields Equation 30.

$$\tau_{xy} = \left[\frac{8m^2n^2}{S_{Lt}^2} + \frac{4m^2n^2}{S_{Tt}^2} + \frac{(m^2 - n^2)^2}{S_s^2} \right]^{-\frac{1}{2}} \quad 29$$

The over shear strength in CSPSW, due to FRP, was achieved by integration of Eq. (29) over the FRP area that yield Eq. (30).



$$F_{frp} = \left[\frac{8m^2n^2}{S_{Lt}^2} + \frac{4m^2n^2}{S_{Tt}^2} + \frac{(m^2 - n^2)^2}{S_s^2} \right]^{-\frac{1}{2}} bt \quad 30$$

FRP ELASTIC SHEAR DISPLACEMENT

To evaluate FRP in CSPSW, Elastic displacement must be determined. For this reason, the internal strain energy in material and the work done by external shear force must be equal. Strain energy density function is stated as Eq. (31).

$$U_0 = \frac{m^4 \sigma_{11}^2}{2E_{xx}} + \frac{n^4 \sigma_{11}^2}{2E_{yy}} + \frac{m^2 n^2 \sigma_{11}^2}{2G_{xy}} \quad 31$$

Strain energy in FRP layer written as Eq. (32).

$$U_{strain\ energy} = \iiint U_0 dV \quad 32$$

After integrating Eq. (32) over the volume in which energy is stored, the strain energy is obtained, Eq. (33).

$$U_{SE} = \left(\frac{m^4 \sigma_{11}^2}{2E_{xx}} + \frac{n^4 \sigma_{11}^2}{2E_{yy}} + \frac{m^2 n^2 \sigma_{11}^2}{2G_{xy}} \right) bdt \quad 33$$

The work done by external shear force state as Eq. (34).

$$W_{shear\ force} = 1 / 2 F_{frp} U_{frp} \quad 34$$

Putting Eq. (33) and Eq. (34) equal, gives the Elastic shear displacement, Eq. (35).

$$U_{frp} = \left(\frac{m^4}{E_{xx}} + \frac{n^4}{E_{yy}} + \frac{m^2 n^2}{G_{xy}} \right) \frac{\sigma_{11}^2 bdt}{F_{frp}} \quad 35$$

Substituting Eq. (30) in Eq. (35) yields the Elastic shear displacement, Eq. (36).

$$U_{frp} = \left(\frac{m^4}{E_{xx}} + \frac{n^4}{E_{yy}} + \frac{m^2 n^2}{G_{xy}} \right) * \left(\frac{8m^2 n^2}{S_{Lt}^2} + \frac{4m^2 n^2}{S_{Tt}^2} + \frac{(m^2 - n^2)^2}{S_s^2} \right)^{\frac{1}{2}} \sigma_{11}^2 d \quad 36$$

In Elastic state, $\sigma_{11} = S_{Lt}$.

RESULTS AND DISCUSSION

Three specimens that have one story steel plate shear wall have been considered to evaluate the effects of FRP on maximum strength and behavior of composite SPSW. The dimensions and boundary element of these specimens are shown in table 1. The connections in frame are rigid. SPSW strengthened is with two layers of FRP, one layer in each side. Thickness of each layer is 0.5 mm.



Table.1 CSSW Dimensions and Sections

	b (m)	d (m)	t (mm)	beam	column
CSSW1	3.2	1.7	4	W10x39	W10x39
CSSW2	3.3	2.3	5	W10x45	W10x45
CSSW3	2	2.9	5	W10x49	W10x49

Table.2 FRP mechanical properties

	E11 (GPA)	E22 (GPA)	G12 (GPA)	v12
	140	10	5	0.28
S _{Lt} (MPa)	S _{Tt} (MPa)	S _{Tc} (MPa)	S _s (MPa)	S _{Lc} (MPa)
1500	50	250	70	1200

FRP materials are tabulate in table 2. The materials considered for frame and plate are conventional steel with $f_y=240$ MPA and $f_u=370$ MPA. Fiber orientation angle is measured in respect to horizontal and increases from 0– 90 degrees to investigate over strength due to FRP layers. Optimum fiber angle as mentioned earlier is in diagonal tension field. Tension field angle is based on Thorburn (1983) and et al and is formulated as Eq.37. Although α is measured in respect to vertical axis, since in this article, the base angle is measured in respect to horizontal axis, tension field angle is $\theta = \pi / 2 - \alpha$.

$$\tan^4 \alpha = (1 + \frac{t_w L}{2A_c}) / (1 + t_w h [\frac{1}{A_b} + \frac{h^3}{360I_c L}]) \quad 37$$

Tension field angle has been calculated for each specimen and is shown in table 3. To evaluate steel shear wall without FRP, PFI method has been considered (Roberts 1991).

Table.3 Tension Field Angle

	CSSW1	CSSW2	CSSW3
α (deg)	35.59	40.89	50.63

Table.4 Parameters of PFI Push-over curve

	F _{pl} (KN)	D _{pl} (mm)	F _{fr} (KN)	D _{fr} (mm)
SSW1	1847.1	4.22	379.2	4.62
SSW2	1933.9	5.41	329.6	8.2
SSW3	1176.9	6.76	295.1	12.61

Using PFI method (Roberts 1991) and Eq. (30) and Eq. (36), parametric push curve for steel plate without FRP, strengthened with FRP, is achieved and has been compared to FEM curves. The superposition pushover curve for composite steel plate shear wall is shown in Fig. 4. In PFI method, tension field angle considered as optimum fiber angle of FRP material. Calculations of PFI parameter are summarized in table 4. Also critical shear buckling stress has been neglected. Over strength due to FRP on SSW has been calculated for three specimens and superposition with PFI curves, because Eq. (30) and Eq. (37) achieved in elastic region superposition are valid. Overall force-displacement of composite shear wall for each specimen is shown in Figs. 3-5 and these curves are compared with FEM pushover curves.

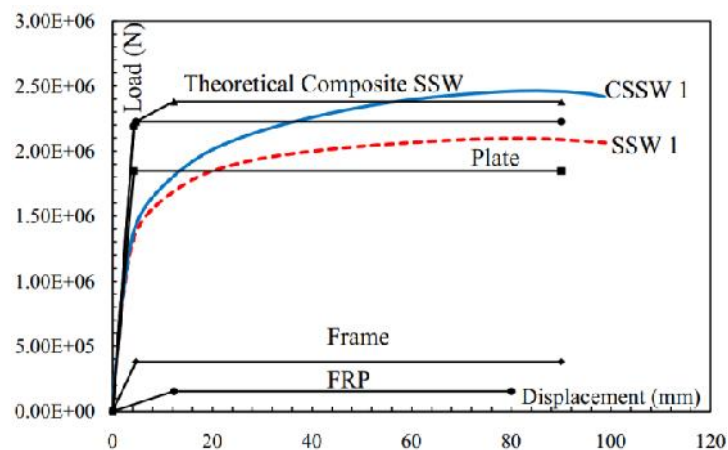


Fig. 3 Theoretical curve for composite SSW1 and FEM Simulation

As shown in figs. 3– 5, the theoretical Eq. (30) and Eq. (36) for predicting FRP elastic displacement and over shear strength are completely consistent with FE models.

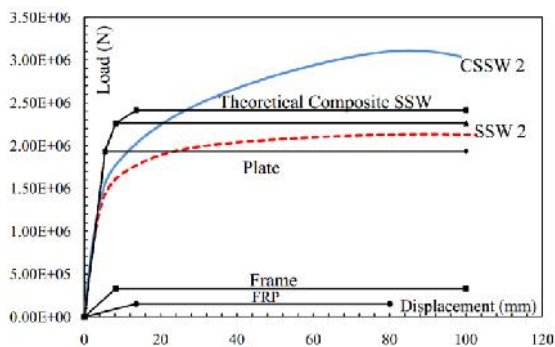


Fig. 4 Theoretical curve for composite SSW2 and FEM Simulation

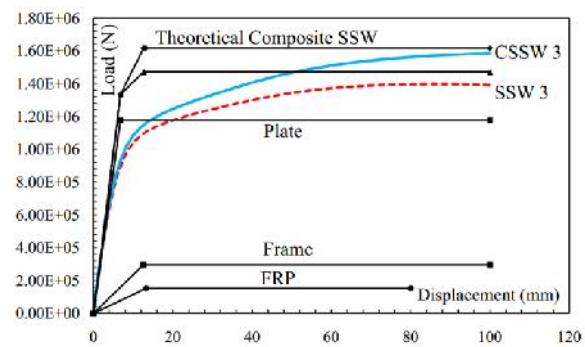


Fig. 5 Theoretical curve for composite SSW3 and FEM Simulation

CONCLUSION

- Using composite structural analysis, some Equations are obtained for elastic shear strength and elastic shear displacement for composite steel shear walls.
- Optimum fiber direction is on tension diagonal tension field in plate In failure criteria in composite materials, Azai-Tsai-Hill yields the most reliable estimate
- for shear strength and maximum stress Criterion yields the most reliable estimate for Elastic shear displacement.
- Using stress – strain Eqs. (3) - (19) given in this article, stress and strain can be obtained in arbitrary direction in FRP material.

REFERENCES

- Astaneh-AslA (2002) Seismic Behavior and Design of Composite Steel Plate Shear Walls, Steel Tips, Structural Steel Educational Council, Technical Information & Product Service, May
- Wagner H (1931) Flat Sheet Metal Girders with Very Thin Webs, Tech No. 604, National Advisory Committee for Aerodynamics, Washington, DC
- Takahashi Y, Takemoto Y, Takeda T and Takagi M (1973) Experimental Study on Thin Steel Shear Walls and Particular Bracing under Alternative Horizontal Load, Preliminary Report. Lisbon, Portugal, pp 185-191
- KharraziMHK (2005) Rational Methods for Analysis and Design of Steel Plate Shear Walls, PhD Dissertation, University of British Columbia
- VianD and BruneauM (2004) Testing of Special LYSS Steel Plate Shear Walls, *13th World Conference on Earthquake Engineering*, Report No. 978, Canada
- RahaA and HatamiF (2009) Evaluation of composite shear wall behavior under cyclic loadings, *Journal of Constructional Steel Research*, 65, 1528-1537
- Arabzadeh A, Soltani M and AyaziA (2011) Experimental investigation of composite shear walls under shear loadings, *Thin-Walled Structures*, 49, 842-854
- Thorburn LJ, Kulak GL and Montgomery CJ (1983) Analysis of Steel Plate Shear Walls. *Structural Engineering Report No. 107*
- RobertsTM and Sabouri-Ghomi S (1991) Hysteretic Characteristics of Unstiffened Plate Shear Panels, *Thin-Walled Structures*, 12, 145-162
- Hahtami F, Ghamari A and Rahai A (2012) Investigating the properties of steel shear walls reinforced with Carbon Fiber Polymers (CFRP), *Journal of Constructional Steel Research*, 70, 36-42
- Nateghi-AlahiF and Khazaei-PoulM (2012) Experimental study of steel plate shear walls with infill plates strengthened by GFRP laminates, *Journal of Constructional Steel Research*, 78, 159-172

